
# pH-dependent absorption spectra of rhodopsin mutant E113Q: On the role of counterions and protein

Peng Xie, Panwang Zhou, Ahmed Alsaedi, Yan Zhang

PII: S1386-1425(16)30669-2
DOI: doi: 10.1016/j.saa.2016.11.015
Reference: SAA 14775

To appear in:

Received date: 21 July 2016
Revised date: 8 November 2016
Accepted date: 12 November 2016

Please cite this article as: Peng Xie, Panwang Zhou, Ahmed Alsaedi, Yan Zhang, pH-dependent absorption spectra of rhodopsin mutant E113Q: On the role of counterions and protein, (2016), doi: 10.1016/j.saa.2016.11.015

# pH-Dependent Absorption Spectra of Rhodopsin Mutant E113Q: On the Role of Counterions and Protein

**Peng Xie,[a] Panwang Zhou,[a] Ahmed Alsaedi,[b] and Yan Zhang[a]***

[a]*State Key Laboratory of Molecular Reaction Dynamics, Dalian Institute of Chemical Physics, Chinese Academy of Sciences, Dalian, Liaoning, People's Republic of China, 116023*
[b]*Nonlinear Analysis and Applied Mathematics (NAAM) Research Group, Department of Mathematics, Faculty of Science, King Abdulaziz University, Jeddah, Saudi Arabia, 21589*

## Abstract

The absorption spectra of bovine rhodopsin mutant E113Q in solutions were investigated at the molecular level by using a hybrid quantum mechanics/molecular mechanics (QM/MM) method. The calculations suggest the mechanism of the absorption variations of E113Q at different pH values. The results indicate that the polarizations of the counterions in the vicinity of Schiff base under protonation and unprotonation states of the mutant E113Q would be a crucial factor to change the energy gap of the retinal to tune the absorption spectra. Glu-181 residue, which is close to the chromophore, cannot serve as the counterion of the protonated Schiff base of E113Q in dark state. Moreover, the results of the absorption maximum in mutant E113Q with the various anions ($Cl^-$, $Br^-$, $I^-$ and $NO_3^-$ ) manifested that the mutant E113Q could have the potential for use as a template of anion biosensors at visible wavelength.

**KEYWORDS** Spectra tuning; QM/MM; E113Q rhodopsin; Hydrogen-bond; Anion biosensor

## 1. Introduction

Rhodopsin from vertebrate eye is a dim-light sensitive receptor protein which belongs to the G protein-coupled receptors (GPCR) family[1-3]. Rhodopsin contains a chromophore (11-*cis* retinal) and protein moiety opsin. Opsin is a seven helical transmembranes protein, and 11-*cis* retinal located in a central pocket on transmembrane helix H7 is covalently tied to the lysine residue through a protonated Schiff base (PSB) linkage[4-7](Figure 1a). The retinal molecule consists of a $\beta$-ionone ring and the Schiff base linked through a polyene chain (Figure 1b). The chromophore (protonated 11-*cis* retinal) absorbs at *ca*. 600 nm in gas-phase [8,9], while the absorption peaks at *ca*. 500 nm in the bovine rhodopsin protein environment[10, 11].

The absorption maximum of wild type rhodopsin is insensitive to pH value of solutions within a wide range, and it can remain 500 nm from pH 3.3 to 8.8 in the solution[12]. Zhukovsky *et al.*[13] and Sakmar *et al.*[14] demonstrated that E113 can interact with the protonated Schiff base of the chromophore as the counterion

* Corresponding author. Tel: +86-411-84379483, Fax: +86-411-84675584
*E-mail address:* zhangyanhg@dicp.ac.cn.

through a series of site-directed mutagenesis experiments. The protonated Schiff base is quite stable with the interaction of Glu-113 in wild type rhodopsin. Site 113, which is the only difference between the mutant E113Q and wild type rhodopsin, is located on the third transmembrane helix near the extracellular surface[15]. When glutamic acid-133 was replaced by glutamine, the E113Q mutant manifested a dramatic pH-dependent equilibrium of protonated and unprotonated retinylidene Schiff base forms. At pH 3.3, the absorbing species of E113Q was completely a PSB form ($\lambda_{max}$ = 490 nm), while only unprotonated Schiff base (SB) form ($\lambda_{max}$ = 380 nm) existed when pH value was great than or equal to 7.2. Two forms coexisted from pH 3.3 to pH 7.2[13, 14]. This conversion between PSB and SB forms in E113Q implies that $H^+/OH^-$ in the solution could get into the opsin and interact with the chromophore. Without competition of the negative charge of E113, other anions in solution may approach the chromophore and affect the absorption spectra.

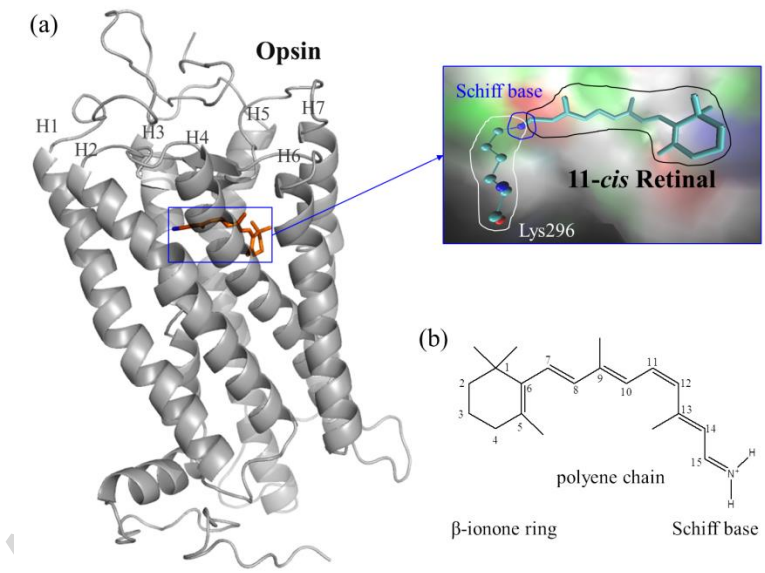


Figure 1. (a) The seven transmembrane helices (H1-H7) of the opsin in the X-ray structure of bovine rhodopsin (PDB code: 1U19[7]). The 11-*cis* retinal's location is shown in blue box. (b) Schematic representation of protonated 11-*cis* retinal.

Compared with the wild type rhodopsin, the mutant E113Q loses one negative charge which can serve as the counterion of PSB at the 113 site. Zhukovsky *et al.*[13] and Sakmar *et al.*[14] supposed the PSB of E113Q may recruit an anion ($Cl^-$) from the solution as the counterion. $Cl^-$ binding with H181 can regulate the absorption maximum in human red and green colour vision pigments mutant E181H. [16] For bovine rhodopsin mutant E113Q, the ion's location and the ion effects on the absorption spectra in solution are still ambiguous so far. Further, the counterion role in most investigations of solvated absorption spectra is seldom elucidated based on our knowledge. As the high-resolution crystal structure of bovine rhodopsin

was reported[7], theoretical computations become possible to provide a deep comprehension of the mechanism through which counterions affect the absorption spectra of bovine rhodopsin and its mutants at the molecular level. In this work, we investigated protonation/deprotonation states of Schiff base and counterion effects on the absorption spectra of rhodopsin mutant E113Q in the dark state by the density functional theory (DFT)[17] and a hybrid quantum mechanics/molecular mechanics (QM/MM) approach in own *N*-layer integrated molecular orbital plus molecular mechanics (ONIOM) scheme.[18, 19]

## 2. Methods

The calculation models of wild type rhodopsin and its mutant E113Q were based on the 2.2 Å resolution X-ray structure of bovine rhodopsin (PDB code: 1U19)[7]. E181 is uncharged state unless otherwise specified. In principle, the phospholipid bilayer should be included in the rhodopsin models. Considering the spectral measurements were performed in an aqueous environment without phospholipid bilayer (using surfactant to stabilize the protein structure) [13, 14], all computational models were set in an octahedral water box by using TIP3P water model[20] with no phospholipid bilayer for model simplification. To keep the protein shape of rhodopsin, we added one disulphide bond between C110 and C187 and kept all salt bridge (such as H195~E197, E232~R252, K231~E239, E247~R135, E341~H65). The protein shape basically remained similar in the short time MD simulations. In the later calculations, the computational results of the first vertical excitation energy of wild type rhodopsin can well reproduce the experimental results. This approximation is proved to be available. The systems were first relaxed to remove conflicts overlaps with atoms by energy minimization, then heated up from 0 K to 300 K in 200 ps by Langevin temperature controls with weak restrain (10 kcal/mol) on the solute at constant volume periodic boundary conditions. Finally, a further 6.0 ns of molecular dynamics were followed without restraints at 300 K at constant pressure (1 atm) with AMBER parm10 force field which includes ff99SB[21] force field for proteins, ff99bsc0[22] force field for DNA, OL3[23] force field for RNA and default parameters for counterions. After each system reached equilibrium, the structure with the lowest energy in the 50 random snapshots taken from the last 1 ns equilibrated MD trajectory was used as the initial geometry of B3LYP/6-31G(d):AMBER10 optimization according to the ONIOM scheme with electronic embedding (EE)[24]. Water molecules 10.0 Å away from amino acid residues were removed. The QM model part consisted of the 11-*cis* retinylidene and $NH_2^+$(protonated state)/NH(unprotonated state) moiety of the side chain of lysine 296. This setting for QM region has been proved dependable by Altun et al.[25] In MM region, the residues within 4.0 Å and water within 6.0 Å from the QM region were relaxed during optimization, and other residues and water molecules were fixed to keep the shape of the protein [for more details, see SI section I and II]. The first vertical excitation energies ($S_0 \rightarrow S_1$) on these structures were calculated by using the SORCI+Q/6-31G(d):AMBER10 method.[20, 26] Many high-level approaches are nowadays available, but

they are limited in application due to the enormous computations. It is desirable to choose one method which can reduce the computational effort while keep reasonable accuracy. Altun et al. [25] reported that SORCI+Q method can reproduce the experimental absorption maxima of retinal very well with acceptable time-consuming. In SORCI+Q calculations, the basis set 6-31G(d) shows better performance than the larger basis sets, and the active space 3-root CAS(6,6) can balance the accuracy and efficiency of calculation compared with the active space CAS(12, 12). Further details of this methodology were given in the SI section III. The MD, ONIOM optimization and vertical excitation energy calculations were carried out with the AMBER 11[27], Gaussian 09 D01[28] and ORCA 3.02[29] program package, respectively.

## 3. Results and Discussions

The computational first vertical excitation energies ( $S_0 \rightarrow S_1$ ) are 584 nm in gas phase, and 496 nm in protein environment at SORCI+Q/6-31G(d): AMBER10 level for wild type bovine rhodopsin. The results of the experiment in gas phase are 600 nm [8,9] and 500 nm in protein environment [10, 11]. The computations reproduce the experimental measurements. Moreover, the calculations at present level reveal better stability (the absorption maxima are blue-shifted at both gas phase and protein environment) than that at other levels (one absorption maxima is blue-shifted while another is red-shifted) calculated by Altun, Sekharan *et al.* [30, 31] as shown in Supporting Information (SI) section V. Therefore, the SORCI+Q/6-31G(d): AMBER10 level was used in the further investigation of spectral computations for E113Q. The limitations of the model and the deficiencies of this treatment were well estimated in previous studies [32, 33], and these investigations indicated that the calculations at present level can give accurate results due to the cancellation effects of the physical models and calculation methods. By using this level, the computed first vertical excitation energies $S_0 \rightarrow S_1$ for both PSB and unprotonated SB states of rhodopsin mutant E113Q (namely PSBR and SBR shown in Figure 2b-e) are 577 nm and 344 nm respectively. In wild type rhodopsin, the hydroxyl of E113 directly forms one H-bond with the PSB. Water 355 is away from PSB and forms a H-bond network with E113 and T94 (Figure 2a). When E113 is replaced with Q113, Q113 moves away from PSB and Water 355 forms H-bond with PSB. A new H-bond network is formed by W355, G90 and T94 around PSB (Figure 2b). The missing of negative charge and the variation of H-bond network red-shift the first vertical excitation energy by 81 nm from 496 nm for wild type to 577 nm for PSBR. Meanwhile, the experimental results are 490 nm for PSBR and 380 nm for SBR[13, 14]. Obviously, these large relative discrepancies between the calculations and experiments could not mainly come from the computational method. Because all experimental measurements were carried out in solution which contained counterions, the absence of counterions could be likely to cause these errors. There are two possibilities for PSB in E113Q to capture the counterions: one is the charged E181 in the neighborhood of

site 113 although E181 is set as uncharged state by default, and the other is anion from the solution.

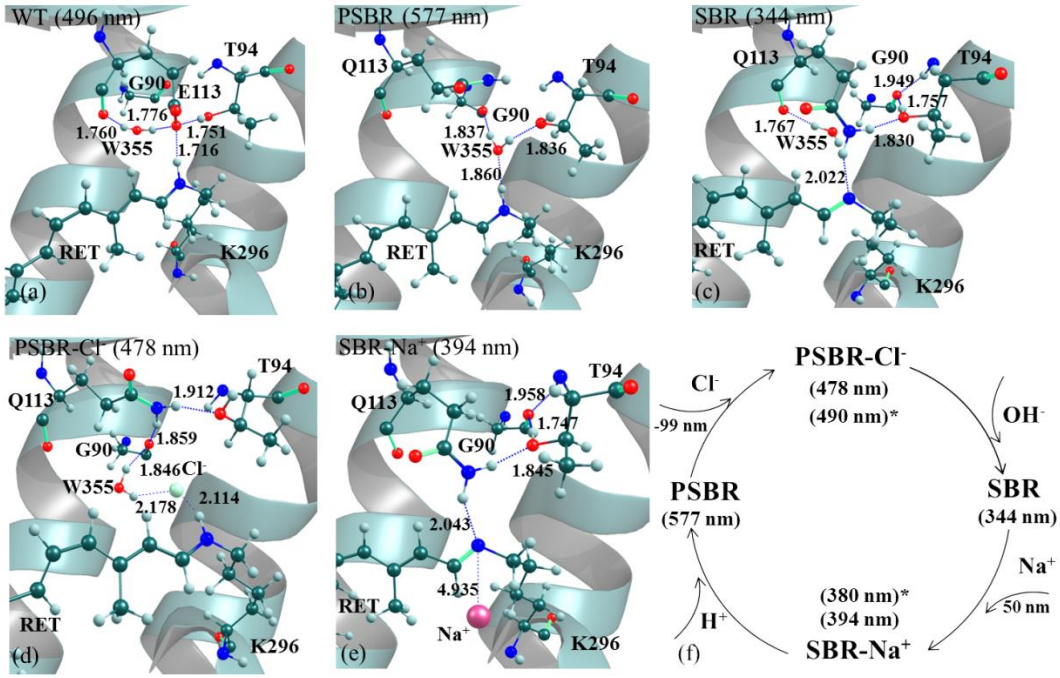


Figure 2. QM/MM optimized geometries of wild type rhodopsin and its mutant E113Q: (a) wild type (WT), (b) protonated state (PSBR), (c) unprotonated state (SBR), (d) PSBR with $Cl^-$ (PSBR-$Cl^-$) and (e) SBR with $Na^+$ (SBR-$Na^+$). (f) Schematic representation of the absorption spectra variations of rhodopsin mutant E113Q in solutions. All distances are in Å. $\lambda_{max}$ with asterisk are the experimental values.

**The state of E181 in E113Q:** E181 lies on the extracellular loop 2 and is close to the polyene chain (C11=C12) of the retinal. In invertebrate rhodopsin E181 is found to be charged state[34]. In contrast, the ionization state of E181 in vertebrate rhodopsin has been a controversial topic for years[35-45]. Some experimental studies assigned E181 as neutral state in rhodopsin through two-photon spectroscopy[35] and pre-resonance Raman spectroscopy[39]. Through a high-level quantum chemical investigation, Sekharan *et al.*[46] concluded that E181 is uncharged in the dark state of vertebrate rhodopsin. In E113Q, can E181 lose one proton and compensate for E113? After optimizing the structures of PSBR of E113Q with charged E181 (PSBR/chE181) (shown in Figure 3a), we found the distance between the carboxyl of E181 and the N of PSB is about 9 Å. It is too far to neutralize the positive charge of PSB, and the H-networks around the PSB are basically invariable. The computed $\lambda_{max}$ of PSBR/chE181 is 549 nm. Although it blue-shifts 28 nm compared with PSBR (577 nm) with the effect of charged E181, the $\lambda_{max}$ still cannot reproduce the experimental value (490 nm). It implies that the charge of E181 could not be responsible for the big difference of PSBR absorption spectra between the computations and experiments. Since all measurements

of absorption spectra for E113Q were measured in solution, it is reasonable to add the counterions in the vicinity of the chromophore. $Cl^-$ can be conducted through a light-gated ion channel in an anion-conducting channelrhodopsin, i.e. a subfamily of rhodopsin. It is also found that the permeability sequence is $NO_3^- > I^- > Br^- > Cl^-$ in this anion-conducting channelrhodopsin.[47] The structure of E113Q is similar as that of anion-conducting channelrhodopsin, so $Cl^-$ could enter the protein and be captured by PSB in E113Q. We optimized the geometries of the PSBR E113Q with $Cl^-$ (namely PSBR-$Cl^-$ shown in Figure 2d) and SBR E113Q with $Na^+$ (namely SRB-$Na^+$ shown in Figure 2e) by ONIOM-EE method. At the optimized geometries, the $S_0 \rightarrow S_1$ energies of PSBR-$Cl^-$ and SBR-$Na^+$ were calculated. The computational absorptions ( $\lambda_{max}$ ) are 478 nm for PSBR-$Cl^-$ and 394 nm for SBR-$Na^+$. These values agreed quite well with the experimental results[13, 14] (490 nm for PSBR and 380 nm for SBR). The $\lambda_{max}$ of PSBR-$Cl^-$ in charged E181 state (PSBR-$Cl^-$/chE181 shown in Figure 3b) is 472 nm. The effect of the E181 charge is only 6 nm and very small in the presence of counterion $Cl^-$. Thus, we considered that the charged E181 could not serve as the counterion of PSB of E113Q in the dark state, and uncharged E181 would be adopted in further calculations.

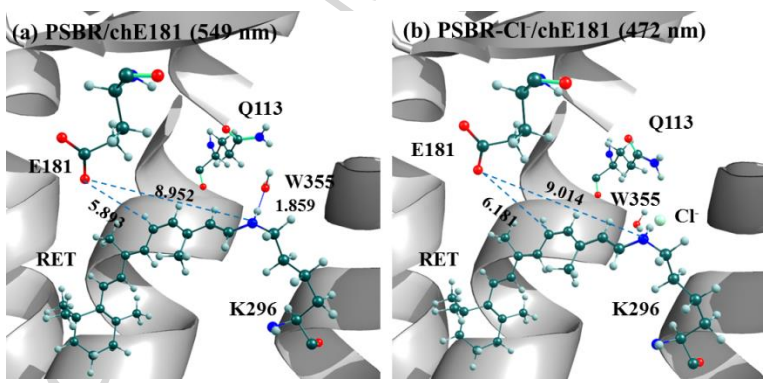


Figure 3. QM/MM optimized geometries of PSB state E113Q with charged state E181: (a) without $Cl^-$ (PSBR/chE181) and (b) with $Cl^-$ (PSBR-$Cl^-$/chE181). All distances are in Å.

**$Cl^-$ effects for PSBR:** $Cl^-$ blue-shifts the first vertical excitation energy by 99 nm from 577 nm for PSBR to 478 nm for PSBR-$Cl^-$. Generally speaking, the electronegativity of chlorine atom is not enough to form hydrogen bond. But in this case, the full negative charge and the lone pairs of $Cl^-$ make it is possible that $Cl^-$ can form one hydrogen bond with the $H^+$ which is attached to the highly electronegative N atom of PSB. In the presence of $Cl^-$, the H-bond between the O of water 355 and the PSB (Figure 2b) is broken. Instead, the $Cl^-$ forms one H-bond with the PSB and another with water 355 (Figure 2d). Obviously, $Cl^-$ has a stronger H-bond with PSB than water 355. Water 355 moves to the polyene side of retinal and H-bonds to $Cl^-$ and G90. The OH of T94 moves away from PSB and forms a new H-bond with the $NH_2$ of glutamine 113.

**Deprotonation effects for PSBR:** After deprotonation of PSBR, the structure of SBR remarkably changes (Figure 2e). In SBR, the $NH_2$ of glutamine directly H-bonds to the N of Schiff base instead of water 355. The H-bond network among PSB, water 355, G90 and T94 in PSBR crashes when water 355 moves away from the Schiff base due to the deprotonation. These structure changes induced the blue shift of the absorption spectra from 577 nm of PSBR to 344 nm of SBR, which could be mainly attributed to the the loss of positive charge in the Schiff base, and the weakening of the H-bond network around the Schiff base would also affect the spectra tuning but it is not the dominating factor[48-50].

**$Na^+$ effects for SBR:** $Na^+$ red-shifts the first vertical excitation energy by 50 nm from 344 nm for SBR to 394 nm for SBR-$Na^+$. In SBR-$Na^+$, $Na^+$ is 4.935 Å away from the Schiff base nitrogen and far from the Q113 site (Figure 2e). By comparing the structures of SBR (Figure 2c) and SBR-$Na^+$ (Figure 2e), it was found that the $Na^+$ changes the location of the amino acid residues around the Schiff base very slightly: the H-bond networks composed by the Schiff base, Q113 and T94 are almost same.

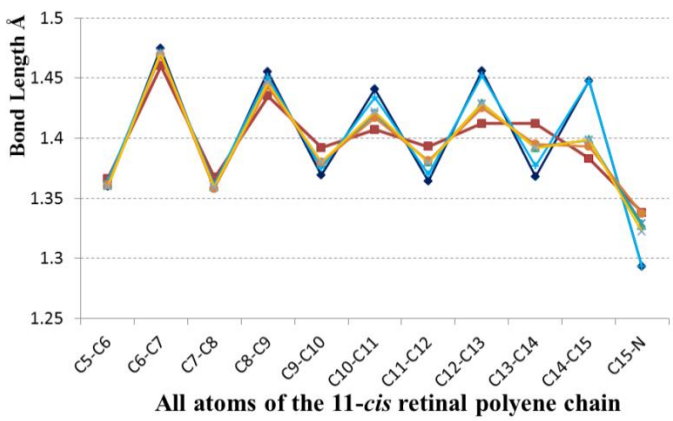


| | BLA | $\lambda_{max}$ |
|---|---|---|
| 1 PSBR | 0.103 | 577 nm |
| 2 SBR | 0.041 | 344 nm |
| 3 SBR-$Na^+$ | 0.095 | 394 nm |
| 4 PSBR-$Cl^-$ | 0.067 | 478 nm |
| 5 PSBR-$Br^-$ | 0.066 | 485 nm |
| 6 PSBR-$I^-$ | 0.061 | 498 nm |
| 7 PSBR-$NO_3^-$ | 0.068 | 470 nm |

Figure 4. Bond lengths (left) along the 11-cis retinal chromophore in optimized QM/MM models of rhodopsin mutant E113Q. The BLA (in Å) and the calculated $\lambda_{max}$ values (right) of each model.

Pal *et al.*[51] proposed the rule that "an increase in BLA is usually correlated with a decrease in $\lambda_{max}$" by analyzing a set of BLA and the corresponding $\lambda_{max}$ of the retinal chromophore in wild type halorhodopsin and its various mutants. The value BLA, i. e. bond length alternation, is defined by the average bond length of single bonds minus the average bond length of double bonds in the C5-$N_{SB}^+$ segment of the retinal chromophore. The similar conclusion were drawn in linear conjugated chromophores in other models such as rhodopsin [52,53] and peridinin [54]. First, we would verify the relationship between the BLA of the retinal chromophore and the $\lambda_{max}$ for seven E113Q models listed in Figure 4. In PSBR, the BLA value is 0.103 Å and the corresponding $\lambda_{max}$ is 577 nm. In PSBR-$Cl^-$, with the strong polarization of $Cl^-$, the BLA decreases to 0.067 Å but the corresponding $\lambda_{max}$ blue-shifts to 478 nm. Accordingly, with the polarization of $Na^+$, the

BLA value in SBR-$Na^+$ increases to 0.095 Å from 0.041 Å in SBR, but the $\lambda_{max}$ of SBR-$Na^+$ red-shifts to 394 nm from 344 nm of SBR. For PSBR and SBR-$Na^+$, although both BLA values are similar, their $\lambda_{max}$ values differ greatly by 50 nm. That is, in the case of the retinal chromophore of E113Q without counterions or in deprotonation state, the rule is not valid. For PSBR-$I^-$, PSBR-$Br^-$, PSBR-$Cl^-$ and PSBR-$NO_3^-$, the BLA values are 0.061 Å, 0.066 Å, 0.067 Å, 0.068 Å and the corresponding $\lambda_{max}$ values are 498 nm, 485 nm, 478 nm, 470 nm respectively. It implies the rule can be verified in this study only when the PSB state retinal chromophore of E113Q interacted with counterions such as $Cl^-$, $Br^-$, $I^-$ and $NO_3^-$. It seems that the BLA value of the retinal chromophore which reflects its configuration correlates with the $\lambda_{max}$ of E113Q to a limited extent, that rule cannot be valid when the environment electrostatics of the chromophore change.

The environment of the retinal chromophore including protein with water and counterions could be responsible for the spectral tuning of E113Q. So far there are some questions that we are still in the dark about, like which part would be primarily responsible, and how to tune the spectra. To answer these questions, we evaluated the protein and counterions contributions for four E113Q models at their respective B3LYP/6-31G(d):AMBER10 optimized ground state geometries (shown in table 1).

*Table 1.* The First Vertical Excitation Energy (in nm) at SORCI+Q/6-31G(d):AMBER10 level of bovine rhodopsin mutant E113Q with/without counterion at B3LYP/6-31G(d):AMBER10 Optimized Ground State Geometries.

| | Retinal | Gas phase | Protein environment | Protein and counterion | experiment |
|---|---|---|---|---|---|
| 1 | PSBR [a] | 609 | 577 | n/a | 490 [e] |
| 2 | PSBR-$Cl^-$ [b] | 601 | 607 | 478 | |
| 3 | SBR [c] | 330 | 344 | n/a | 380 [e] |
| 4 | SBR-$Na^+$ [d] | 339 | 353 | 394 | |

Optimized geometry of [a] protonated state rhodopsin mutant E113Q, [b] protonated state rhodopsin mutant E113Q with $Cl^-$, [c] unprotonated state rhodopsin mutant E113Q and [d] unprotonated state rhodopsin mutant E113Q with $Na^+$. [e] Reference 13 and 14.

**Structure effect of bare retinal chromophore (gas phase):** Through the above BLA analysis (shown in Figure 4), it is found that the structures of the retinal change significantly in PSBR and PSBR-$Cl^-$ due to the polarization of $Cl^-$. Surprisingly, the calculated $\lambda_{max}$ of the bare retinal chromophore (gas phase) of PSBR (609 nm) is very close to that of PSBR-$Cl^-$ (601 nm) (shown in Table 1). The similar phenomena could be observed in models SBR and SBR-$Na^+$. That is, the effect of the structure variation of the bare retinal caused by counterion polarization is very small on the spectral tuning for the dark state E113Q.

**Protein effects:** When the environment only contain the protein with water, $\lambda_{max}$ are 607 nm for PSBR-$Cl^-$, 344 nm for SBR, and 353 nm for SBR-$Na^+$ respectively. Comparing with the $\lambda_{max}$ in gas phase, the

proteins with water red-shift the first vertical excitation energy 6 nm, 14 nm and 14 nm respectively. In contrast, $\lambda_{max}$ of PSBR is 577 nm and the protein with water blue-shifts the first vertical excitation energy by 32 nm. By observing the structures in Figure 2, it could be found that the PSB forms a strong H-bond with water 355 in PSBR while the protein has no H-bond with the PSB in PSBR-$Cl^-$. It is obvious that the polarization of water 355 is important and would affect the first vertical excitation energy of the retinal chromophore. The H-bond formed by PSB (H-bond donor) and water 355 (H-bond acceptor) would be responsible for the blue-shift in PSBR. The polar molecule water 355 would try to play the role of counterion through the H-bond, but it still could not compensate for E113 due to the lack of negative charge. In SBR and SBR-$Na^+$, $Na^+$ has almost no influence on the structure of the amino acid residues around the Schiff base, and both $NH_2$ groups of Q113 similarly H-bond to the Schiff base. It means the H-bond between the Schiff base (H-bond acceptor) and Q113 (H-bond donor) would red-shift the first vertical excitation energy of the retinal chromophore. In general, the protein environment only gives a small contribution to the first vertical excitation energies of the E113Q retinal chromophore. This finding is coincidence with the conclusions proposed by Andruniow et al.[40] and Coto et al.[55]: the protein without counterion induces a red-shift of the chromophore absorption spectra maxima, but the interaction between the chromophore and the protein cavity is very weak.

**Counterion effects:** In PSBR-$Cl^-$, the $Cl^-$ plays the role of counterion for PSB, and the interactions of its negative charge and the H-bond with PSB create a strong polar environment for the retinal chromophore. To examine how counterions affect the first vertical excitation energy of the chromophore, we analyzed the frontier molecular orbitals (HOMO-1 ~ LUMO+1) of the retinal chromophores in PSBR and PSBR-$Cl^-$ (shown in Figure S2a~b shown in SI). Although the orbital shapes substantially do not change, the energy gap ($E_{LUMO}$ - $E_{HOMO}$) increases from 3.89 eV of PSBR to 4.16 eV of PSBR-$Cl^-$. Ultimately, the counterion $Cl^-$ blue-shifts the first vertical excitation energy of the retinal chromophore by 129 nm. By contrast, the $Na^+$ further red-shifts the first vertical excitation energy by 41 nm. The $Na^+$ has little influence on the structure of residues around the Schiff base, but its positive charge would affect the frontier molecular orbitals of the retinal chromophore. It is found that the orbital shapes of SBR and SBR-$Na^+$ (Figure S2c and S5d shown in SI) are similar, but the energy gap decreases from 4.71 eV (SBR) to 4.52 eV (SBR-$Na^+$).

Taken together, the Schiff base segment of the retinal chromophore is the key region to control the spectral tuning in E113Q. The opsin of E113Q would help the retinal chromophore maintain the twisted shape and slightly red-shift the first vertical excitation energy of the retinal chromophore, and the charge polarization of the counterion which surrounds the retinal chromophore would be mainly responsible for the spectral tuning in E113Q.

Based on the above results, the pH dependence of E113Q absorption spectra variations could be considered as shown in Figure 2f. Firstly, in the acid or neutral solution the Schiff base in E113Q could

capture one proton from the solution to form PSBR. Due to the electrostatic interaction, the PSB with the positive charge could attract one $Cl^-$ from solution to form PSBR-$Cl^-$. The $\lambda_{max}$ of PSBR (577 nm) blue-shifts to 478 nm under the influence of $Cl^-$. As the pH value of solution increases, $OH^-$ has more opportunity to approach the PSB to neutralize the proton and form water. $Cl^-$ is released without the bondage of the positive charge of PSB. The $\lambda_{max}$ of SBR further blue-shifts to 344 nm. Actually, the $Na^+$ in solution could move to the vicinity of the retinal chromophore of E113Q without the repulsion of the proton. Then, the positive charge of $Na^+$ red-shifts the $\lambda_{max}$ to 394 nm in SBR-$Na^+$. Lastly, the Schiff base would be protonated again as the pH value of solution decreases.

Meanwhile we noticed that the H-bond between the Schiff base and the counterion also affects the spectral tuning in E113Q. It implies that the absorption spectra of the mutant E113Q would be modulated by regulating the H-bond length between the Schiff base and various counterions, and it becomes possible for E113Q to use as a anion biosensor template.

Since $Cl^-$ could get into the opsin as the counterion of PSB in E113Q, we speculated that other anions with one negative charge could have same effect although they may differ in size and shape. Therefore, we substituted $Cl^-$ with $Br^-$, $I^-$, and $NO_3^-$ to analyze both electrostatic and steric effects on $\lambda_{max}$ of E113Q rhodopsin. This substitutions of anions do not significantly change the locations of amino acid residues and water molecule around PSB. The architecture of the H-bond network in this region basically remains conserved except that the H-bond lengths between the anion and PSB vary from 1.795 Å to 2.580 Å (Figure 5). The $\lambda_{max}$ values computed in these models are listed in the order of: PSBR-$I^-$ (498 nm) > PSBR-$Br^-$ (485 nm) > PSBR-$Cl^-$ (478 nm) > PSBR-$NO_3^-$ (470 nm). It is proportional to H-bond length, PSB-$I^-$ (2.580 Å) > PSB-$Br^-$ (2.388 Å) > PSB-$Cl^-$ (2.114 Å) > PSB-$NO_3^-$ (1.795 Å). The relationship between the H-bond lengths and the $\lambda_{max}$ values are shown in Figure 5d. Generally, the direct H-bond between PSB and the counterion would blue-shift the $\lambda_{max}$, and the $\lambda_{max}$ value would vary inversely with the strength of the H-bond at the visible light region.

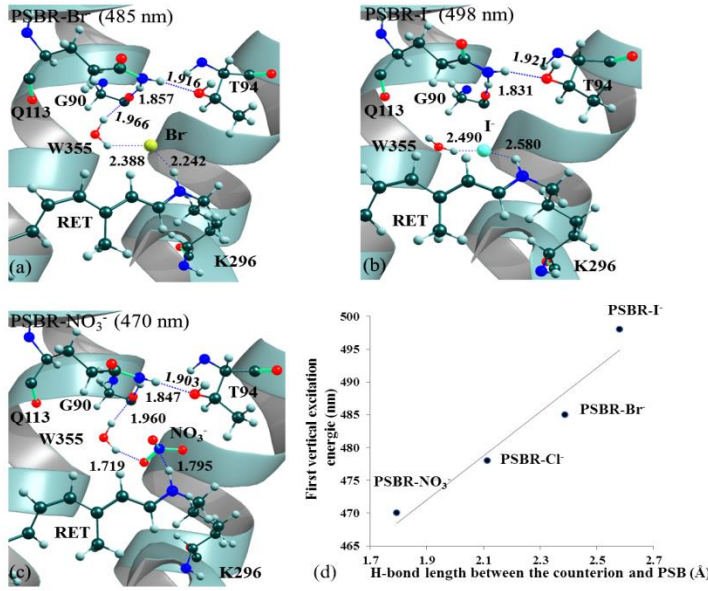


Figure 5. QM/MM optimized geometries of (a) PSBR-$Br^-$, (b) PSBR-$I^-$ and (c) PSBR-$NO_3^-$. (d) The relationship between the H-bond lengths and the first vertical excitation energy values. All distances are in Å.

## 4. Conclusions

In summary, we have investigated structures and the first excitation energies of bovine rhodopsin mutant E113Q in solutions under different acidities by QM/MM calculations. The computations provide a fundamental insight into the origin of the absorption variations of E113Q at different pH values. The contributions of the structure of bare retinal chromophore, opsin and counterion to the spectral tuning were analyzed in detail respectively. It is clear that the absorption spectra would be mainly tuned by the counterions. Anion could blue-shift the absorption peak through increasing the energy gap of the retinal chromophore while cation could red-shift the absorption peak through decreasing the energy gap of the retinal chromophore. The computational absorption spectra with the protein and counterions are in good agreement with the experiments. E181 cannot act as the counterion of PSB in the dark state. The relationship between the $\lambda_{max}$ and anions which directly H-bonds to the PSB of E113Q also implies that E113Q rhodopsin could be a good candidate to produce protein-based chromophoric anion biosensors at visible wavelength.

**Acknowledgements**

This work was supported by a grant from the National Natural Science Foundation of China (21403225 and 21103167).

Additional Supporting Information may be found in the online version of this article.

**References**


1. W. L. Hubbell, M. D. Bownds, Visual transduction in vertebrate photoreceptors, Annu. Rev. Neurosci., 2 (1979) 17-34.
2. S. Filipek, R. E. Stenkamp, D. C. Teller, K. Palczewski, G protein-coupled receptor rhodopsin: A prospectus, Annu. Rev. Physiol., 65 (2003) 851-879.
3. T. P. Sakmar, S. T. Menon, E. P. Marin, E. S. Awad, Rhodopsin: Insights from recent structural studies, Annu. Rev. Biophys. Biomol. Struct., 31(2002) 443-484.
4. D. D. Thomas, L. Stryer, Transverse Location of the Retinal Chromophore of Rhodopsin in Rod Outer Segment Disk Membranes, J. Mol. Biol., 154 (1982) 145-157.
5. E. A. Dratz, P. A. Hargrave, The Structure of Rhodopsin and the Rod Outer Segment Disk Membrane, Trends Biochem. Sci., 8 (1983) 128-131.
6. S. T. Menon, M. Han, T. P. Sakmar, Rhodopsin: Structural basis of molecular physiology, Physiol. Rev., 81 (2001) 1659-1688.
7. T. Okada, M. Sugihara, A.-N. Bondar, M. Elstner, P. Entel, V. Buss, The Retinal Conformation and its Environment in Rhodopsin in Light of a New 2.2Å Crystal Structure, J. Mol. Biol., 342 (2004) 571-583.
8. I. B. Nielsen, L. Lammich, L. H. Andersen, S-1 and S-2 excited states of gas-phase Schiff-base retinal chromophores, Phys. Rev. Lett., 96 (2006) DOI:10.1103/ PhysRevLett. 96. 018304.
9. J. Rajput, A. Hirshfeld, M. Sheves, P. Altoè, G. Orlandi, M. Garavelli, Probing and Modeling the Absorption of Retinal Protein Chromophores in Vacuo. Angew. Chem. 122 (2010), 1834-1837.
10. G. Wald, P. K. Brown, Human rhodopsin, Science, 127 (1958) 222-226.
11. G. Wald, Molecular basis of visual excitation, Nature, 219 (1968) 800-807.
12. C. M. Radding, G. Wald, The stability of rhodopsin and opsin - effects of pH and aging, J. Gen.Phys., 39 (1956) 923-933.
13. E. A. Zhukovsky, D. D. Oprian, Effect of Carboxylic Acid Side Chains on the Absorption Maximum of Visual Pigments, Science, 246 (1989) 928-930.
14. T. P. Sakmar, R. R. Franke, H. G. Khorana, Glutamic acid-113 serves as the retinylidene Schiff-base counterion in bovine rhodopsin, Proc. Natl. Acad. Sci. U.S.A, 86 (1989) 8309-8313.
15. R. R. Birge, Nature of the primary photochemical events in rhodopsin and bacteriorhodopsin, Biochim. Biophys. Acta, 1016 (1990) 293-327.
16. O. P. Ernst, D. T. Lodowski, M. Elstner, P. Hegemann, L. S. Brown, H. Kandori, Microbial and Animal Rhodopsins: Structures, Functions, and Molecular Mechanisms. Chem. Rev., 114 (2014), 126-163.
17. W. Kohn, L. J. Sham, Self-Consistent Equations Including Exchange and Correlation Effects, Phys. Rev., 140 (1965) A1133-A1138.
18. D. Bakowies, W. Thiel, Hybrid models for combined quantum mechanical and molecular mechanical approaches, J. Phys. Chem., 100 (1996) 10580-10594.
19. T. Vreven, K. S. Byun, I. Komaromi, S. Dapprich, J. A. Montgomery, K. Morokuma, M. J. Frisch, Combining quantum mechanics methods with molecular mechanics methods in ONIOM, J. Chem. Theory Comput., 2 (2006) 815-826.
20. D. A. Case, T. E. Cheatham, T. Darden, H. Gohlke, R. Luo, K. M. Merz, A. Onufriev, C. Simmerling, B. Wang, R. J. Woods, The Amber biomolecular simulation programs, J.Comp. Chem., 26 (2005) 1668-1688.

21. V. Hornak, R. Abel, A. Okur, B. Strockbine, A. Roitberg, C. Simmerling, Comparison of multiple amber force fields and development of improved protein backbone parameters, Proteins., 65 (2006) 712-725.
22. A. Perez, I. Marchan, D. Svozil, J. Sponer, T. E. Cheatham, III, C. A. Laughton, M. Orozco, Refinenement of the AMBER force field for nucleic acids: Improving the description of alpha/gamma conformers, Biophys. J., 92 (2007) 3817-3829.
23. P. Banas, D. Hollas, M. Zgarbova, P. Jurecka, M. Orozco, T. E. Cheatham, III, J. Sponer, M. Otyepka, Performance of Molecular Mechanics Force Fields for RNA Simulations: Stability of UUCG and GNRA Hairpins, J. Chem. Theory Comput., 6 (2010) 3836-3849.
24. T. Vreven, K. Morokuma, O. Farkas, H. B. Schlegel, M. J. Frisch, Geometry optimization with QM/MM, ONIOM, and other combined methods. I. Microiterations and constraints, J. Comput. Chem., 24 (2003) 760-769.
25. A. Altun, S. Yokoyama, K. Morokuma, Mechanism of Spectral Tuning Going from Retinal in Vacuo to Bovine Rhodopsin and its Mutants: Multireference ab Initio Quantum Mechanics/Molecular Mechanics Studies, J. Phys. Chem. B, 112 (2008) 16883-16890.
26. F. Neese, A spectroscopy oriented configuration interaction procedure, J. Chem. Phys., 119 (2003) 9428-9443.
27. D. Case, T. Darden, T. Cheatham III, C. Simmerling, J. Wang, R. Duke, R. Luo, R. Walker, W. Zhang, K. Merz, University of California, San Francisco, 2010.
28. M. Frisch, G. Trucks, H. Schlegel, G. Scuseria, M. Robb, J. Cheeseman, G. Scalmani, V. Barone, B. Mennucci, G. Petersson, Gaussian Inc.: Wallingford, CT, USA, 2009.
29. F. Neese, Max-Planck Institute for Bioinorganic Chemistry, Mülheim an der Ruhr, Germany, 2014.
30. A. Altun, S. Yokoyama, K. Morokuma, Spectral tuning in visual pigments: An ONIOM(QM : MM) study on bovine rhodopsin and its mutants, J. Phys. Chem. B, 112 (2008) 6814-6827.
31. S. Sekharan, K. Morokuma, QM/MM Study of the Structure, Energy Storage, and Origin of the Bathochromic Shift in Vertebrate and Invertebrate Bathorhodopsins, J. Am. Chem. Soc., 133 (2011) 4734-4737.
32. O. Valsson, P. Campomanes, I. Tavernelli, U. Rothlisberger, C. Filippi, Rhodopsin Absorption from First Principles: Bypassing Common Pitfalls, J. Chem. Theory Comput., 9 (2013) 2441-2454.
33. S. Gozem, M. Huntress, I. Schapiro, R. Lindh, A. A. Granovsky, C. Angeli, M. Olivucci, Dynamic Electron Correlation Effects on the Ground State Potential Energy Surface of a Retinal Chromophore Model. J. Chem. Theory Comput., 8 (2012), 4069-4080.
34. A. Terakita, T. Yamashita, Y. Shichida, Highly conserved glutamic acid in the extracellular IV-V loop in rhodopsins acts as the counterion in retinochrome, a member of the rhodopsin family, Proc. Natl. Acad. Sci. U.S.A, 97 (2000) 14263-14267.
35. R. R.Birge, L. P. Murray, B. M. Pierce, H. Akita, V. Baloghnair, L. A. Findsen, K. Nakanishi, Two-photon spectroscopy of locked-11-cis-rhodopsin: evidence for a protonated Schiff base in a neutral protein binding site. Proc. Natl. Acad. Sci. U.S.A., 82 (1985), 4117-4121.
36. L. Mollevanger, A. P. M. Kentgens, J. A. Pardoen, J. M. L. Courtin, W. S. Veeman, J. Lugtenburg, W. J. Degrip, High-resolution solid-state C-13-NMR study of carbons C-5 and C-12 of the chromophore of bovine rhosopsin - evidence for a 6-s-cis conformation with negative-charge perturbation near C-12, Eur. J. Biochem., 163 (1987) 9-14.

37. S. O. Smith, I. Palings, M. E. Miley, J. Courtin, H. Degroot, J. Lugtenburg, R. A. Mathies, R. G. Griffin, Solid-state NMR-studies of the mechanism of the opsin shift in the visual pigment rhodopsin, Biochemistry, 29 (1990) 8158-8164.
38. M. Han, S. O. Smith, NMR constraints on the location of the retinal chromophore in rhodopsin and barthorhodopsin, Biochemistry, 34 (1995) 1425-1432.
39. E. C. Y. Yan, M. A. Kazmi, Z. Ganim, J. M. Hou, D. H. Pan, B. S. W. Chang, T. P. Sakmar, R. A. Mathies, Retinal counterion switch in the photoactivation of the G protein-coupled receptor rhodopsin, Proc. Natl. Acad. Sci. U.S.A, 100 (2003) 9262-9267.
40. T. Andruniow, N. Ferre, M. Olivucci, Structure, initial excited-state relaxation, and energy storage of rhodopsin resolved at the multiconfigurational perturbation theory level, Proc. Natl. Acad. Sci. U.S.A, 101 (2004) 17908-17913.
41. J. A. Gascon, V. S. Batista, QM/MM study of energy storage and molecular rearrangements due to the primary event in vision, Biophys. J., 87 (2004) 2931-2941.
42. S. Ludeke, R. Beck, E. C. Y. Yan, T. P. Sakmar, F. Siebert, R. Vogel, The role of Glu181 in the photoactivation of rhodopsin. J. Mol. Biol., 353 (2005), 345-356.
43. G. Tomasello, G. Olaso-Gonzalez, P. Altoe, M. Stenta, L. Serrano-Andres, M. Merchan, G. Orlandi, A. Bottoni, M. Garavelli, Electrostatic Control of the Photoisomerization Efficiency and Optical Properties in Visual Pigments: On the Role of Counterion Quenching. J. Am. Chem. Soc., 131 (2009), 5172-5186.
44. J. S. Frahmcke, M. Wanko, P. Phatak, M. A. Mroginski, M. Elstner, The Protonation State of Glu181 in Rhodopsin Revisited: Interpretation of Experimental Data on the Basis of QM/MM Calculations. J. Phys. Chem. B, 114 (2010), 11338-11352.
45. M. N. Sandberg, T. L. Amora, L. S. Ramos, M. H. Chen, B. E. Knox, R. R. Birge, Glutamic Acid 181 Is Negatively Charged in the Bathorhodopsin Photointermediate of Visual Rhodopsin. J. Am. Chem. Soc., 133 (2011), 2808-2811.
46. S. Sekharan, V. Buss, Glutamic Acid 181 Is Uncharged in Dark-Adapted Visual Rhodopsin, J. Am. Chem. Soc., 130 (2008) 17220-17221.
47. E. G. Govorunova, O. A. Sineshchekov, R. Janz, X. Q. Liu, J. L. Spudich, Natural light-gated anion channels: A family of microbial rhodopsins for advanced optogenetics. Science 349 (2015) 647-650.
48. S. Sekharan, O. Weingart, V. Buss, Ground and excited states of retinal Schiff base chromophores by multiconfigurational perturbation theory, Biophys. J., 91 (2006) L7-L9.
49. S. Sekharan, V. L. Mooney, I. Rivalta, M. A. Kazmi, M. Neitz, J. Neitz, T. P. Sakmar, E. C. Y. Yan, V. S. Batista, Spectral Tuning of Ultraviolet Cone Pigments: An Interhelical Lock Mechanism, J. Am. Chem. Soc., 135 (2013) 19064-19067.
50. G.-J. Zhao, K.-L. Han, Hydrogen Bonding in the Electronic Excited State, Acc.Chem. Res., 45(2011) 404-413.
51. R. Pal, S. Sekharan, V. S. Batista, Spectral Tuning in Halorhodopsin: The Chloride Pump Photoreceptor, J. Am. Chem. Soc., 135 (2013) 9624-9627
52. E. Coccia, D. Varsano, L. Guidoni, Protein Field Effect on the Dark State of 11-cis Retinal in Rhodopsin by Quantum Monte Carlo/Molecular Mechanics. J. Chem. Theory Comput., 9 (2013), 8-12.
53. D.Varsano, E. Coccia, O. Pulci, A. M. Conte, L. Guidoni, Ground state structures and electronic excitations of biological chromophores at Quantum Monte Carlo/Many Body Green's Function Theory level. Comput. Theor. Chem., 1040–1041 (2014), 338-346.
54. E. Coccia, D. Varsano, L. Guidoni, Ab Initio Geometry and Bright Excitation of Carotenoids: Quantum Monte Carlo and Many Body Green's Function Theory Calculations on Peridinin. J. Chem. Theory Comput., 10 (2014), 501-506.

55. P. B. Coto, A. Strambi, N. Ferre, M. Olivucci, The color of rhodopsins at the ab initio multiconfigurational perturbation theory resolution. Proc. Natl. Acad. Sci. U.S.A, 103 (2006), 17154-17159.

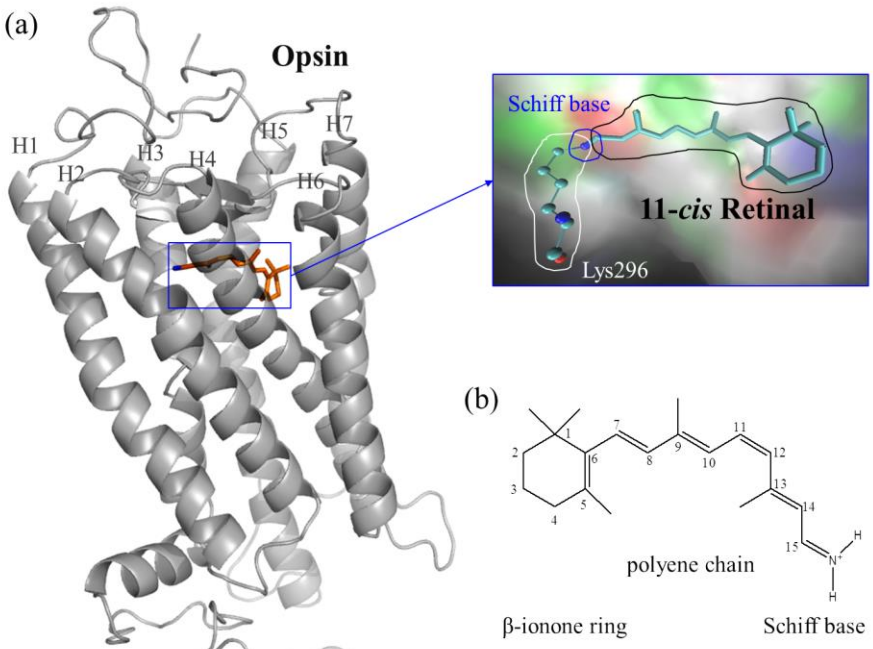


Figure 1

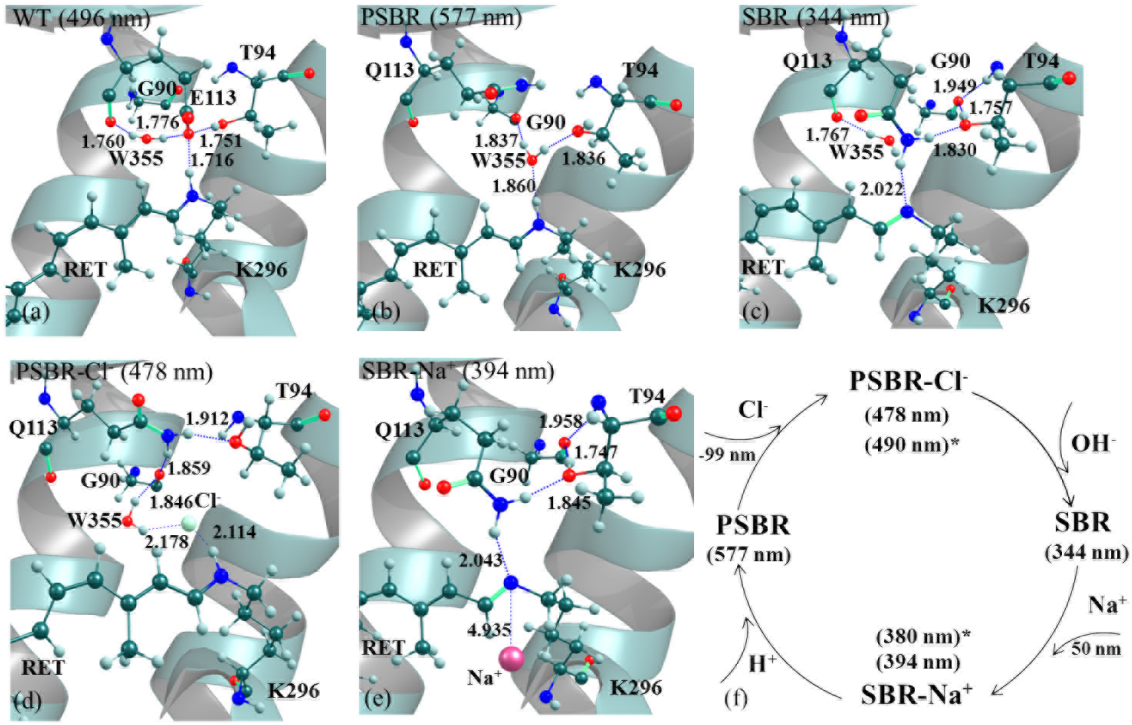


Figure 2

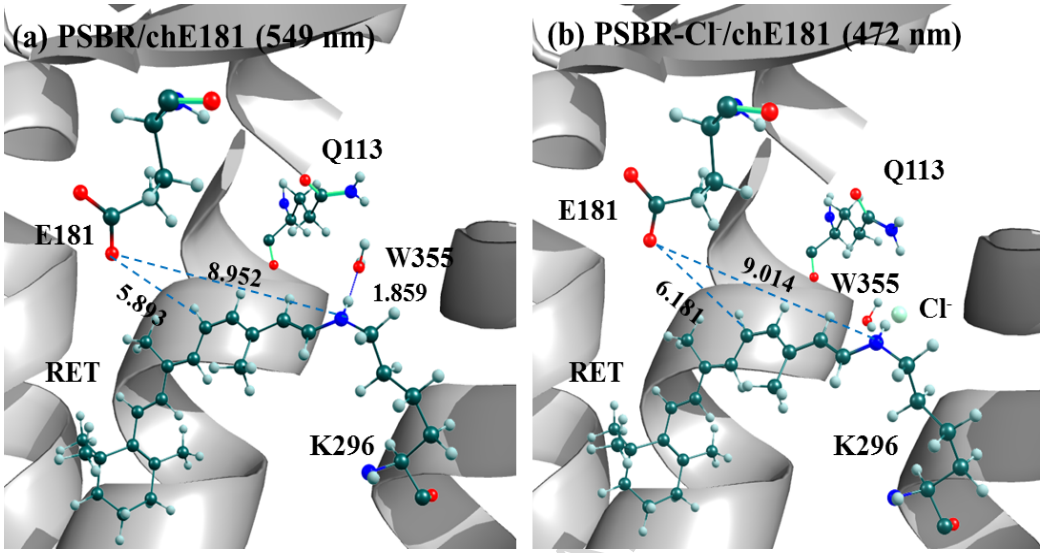


Figure 3

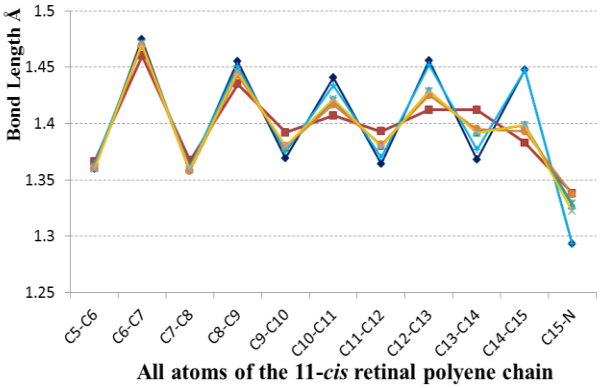


| | BLA | $\lambda_{max}$ |
|---|---|---|
| 1 PSBR | 0.103 | 577 nm |
| 2 SBR | 0.041 | 344 nm |
| 3 SBR-$Na^+$ | 0.095 | 394 nm |
| 4 PSBR-$Cl^-$ | 0.067 | 478 nm |
| 5 PSBR-$Br^-$ | 0.066 | 485 nm |
| 6 PSBR-$I^-$ | 0.061 | 498 nm |
| 7 PSBR-$NO_3^-$ | 0.068 | 470 nm |

Figure 4

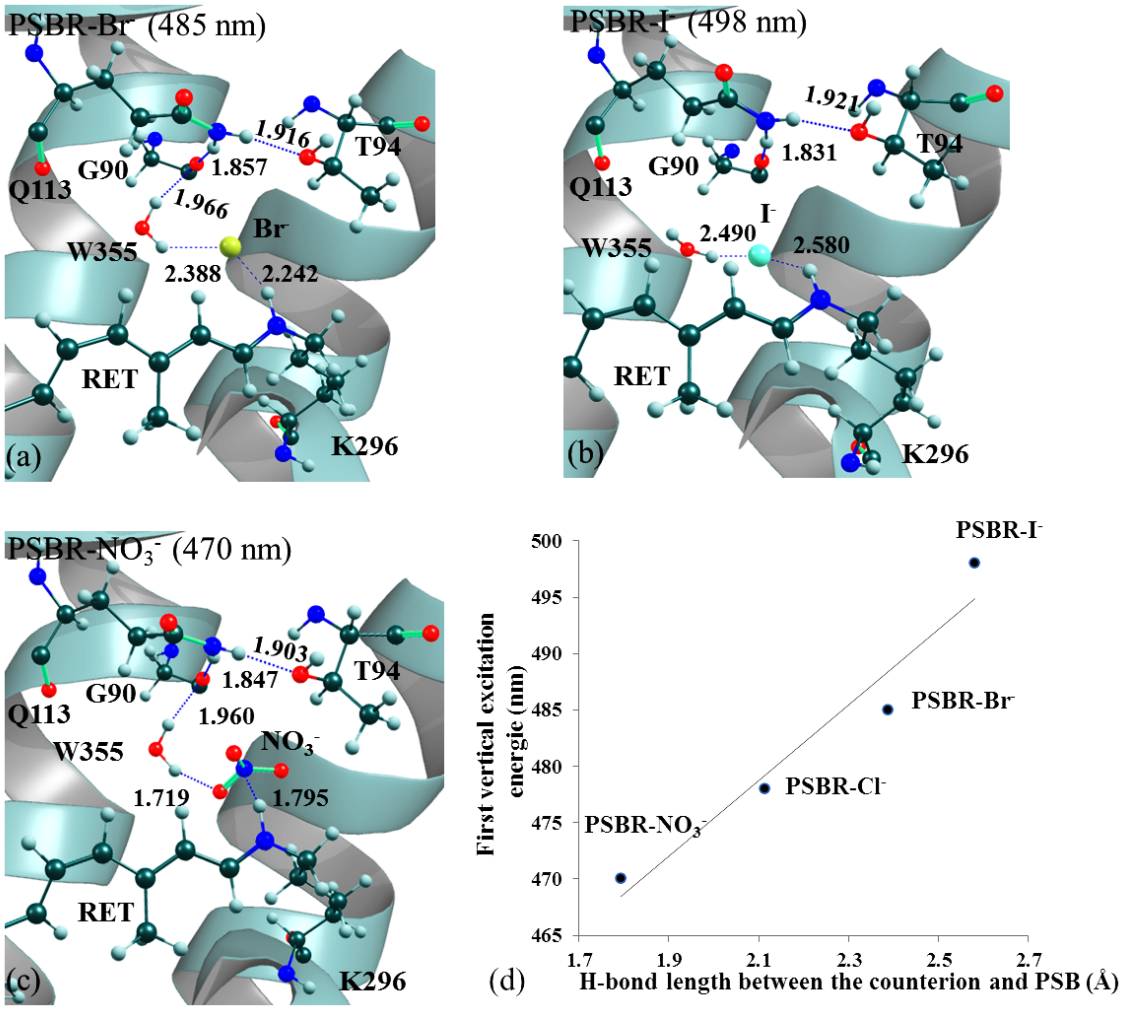


Figure 5

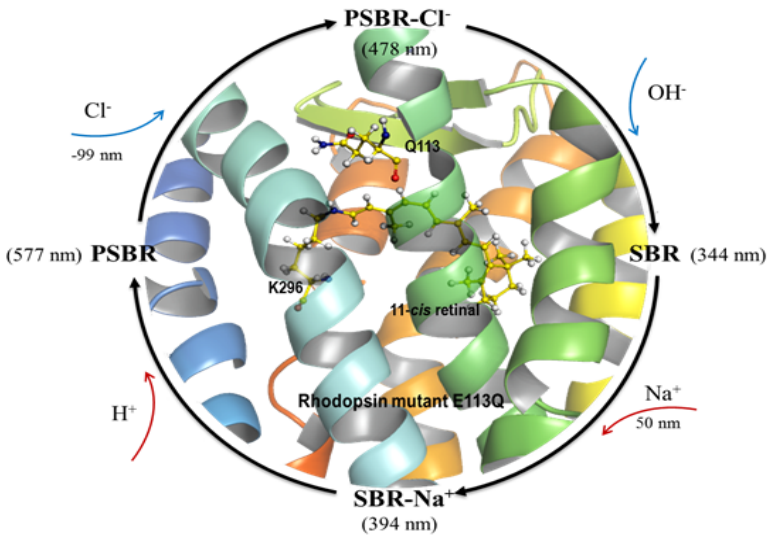


Graphical abstract

**Highlights**

- The absorption spectral tuning mechanism of E113Q rhodopsin in dark state at different pH values is elaborated.
- The counterions in the vicinity of Schiff base are more crucial than the protein environments to affect the absorption spectra of E113Q rhodopsin.
- E113Q rhodopsin has the potential for use as a template of anion biosensors at visible wavelength.